

RESEARCH ARTICLE

Identification and Characterization of Bifunctional Proline Racemase/Hydroxyproline Epimerase from Archaea: Discrimination of Substrates and Molecular Evolution

Seiya Watanabe*, Yoshiaki Tanimoto, Hisashi Nishiwaki, Yasuo Watanabe

Faculty of Agriculture, Ehime University, Matsuyama, Ehime, 790–8566, Japan

* irab@agr.ehime-u.ac.jp



OPEN ACCESS

Citation: Watanabe S, Tanimoto Y, Nishiwaki H, Watanabe Y (2015) Identification and Characterization of Bifunctional Proline Racemase/Hydroxyproline Epimerase from Archaea: Discrimination of Substrates and Molecular Evolution. PLoS ONE 10(3): e0120349. doi:10.1371/journal.pone.0120349

Academic Editor: Paul Taylor, University of Edinburgh, UNITED KINGDOM

Received: October 31, 2014

Accepted: January 21, 2015

Published: March 18, 2015

Copyright: © 2015 Watanabe et al. This is an open access article distributed under the terms of the [Creative Commons Attribution License](https://creativecommons.org/licenses/by/4.0/), which permits unrestricted use, distribution, and reproduction in any medium, provided the original author and source are credited.

Data Availability Statement: All relevant data are within the paper and its Supporting Information files.

Funding: The authors have no support or funding to report.

Competing Interests: The authors have declared that no competing interests exist.

Abstract

Proline racemase (ProR) is a member of the pyridoxal 5'-phosphate-independent racemase family, and is involved in the Stickland reaction (fermentation) in certain clostridia as well as the mechanisms underlying the escape of parasites from host immunity in eukaryotic *Trypanosoma*. Hydroxyproline epimerase (HypE), which is in the same protein family as ProR, catalyzes the first step of the *trans*-4-hydroxy-L-proline metabolism of bacteria. Their substrate specificities were previously considered to be very strict, in spite of similarities in their structures and catalytic mechanisms, and no racemase/epimerase from the ProR superfamily has been found in archaea. We here characterized the ProR-like protein (OCC_00372) from the hyperthermophilic archaeon, *Thermococcus litoralis* (TIProR). This protein could reversibly catalyze not only the racemization of proline, but also the epimerization of 4-hydroxyproline and 3-hydroxyproline with similar kinetic constants. Among the four (putative) ligand binding sites, one amino acid substitution was detected between TIProR (tryptophan at the position of 241) and natural ProR (phenylalanine). The W241F mutant showed a significant preference for proline over hydroxyproline, suggesting that this (hydrophobic and bulky) tryptophan residue played an importance role in the recognition of hydroxyproline (more hydrophilic and bulky than proline), and substrate specificity for hydroxyproline was evolutionarily acquired separately between natural HypE and ProR. A phylogenetic analysis indicated that such unique broad substrate specificity was derived from an ancestral enzyme of this superfamily.

Introduction

L-Proline can serve as a complete source of carbon and energy or of nitrogen for organisms. The metabolism of L-proline is generally initiated through its oxidation by L-proline dehydrogenase (EC 1.5.99.8; L-ProDH) to form Δ^1 -pyrroline-5-carboxylate (Pyr5C) [1] (Fig. 1A).

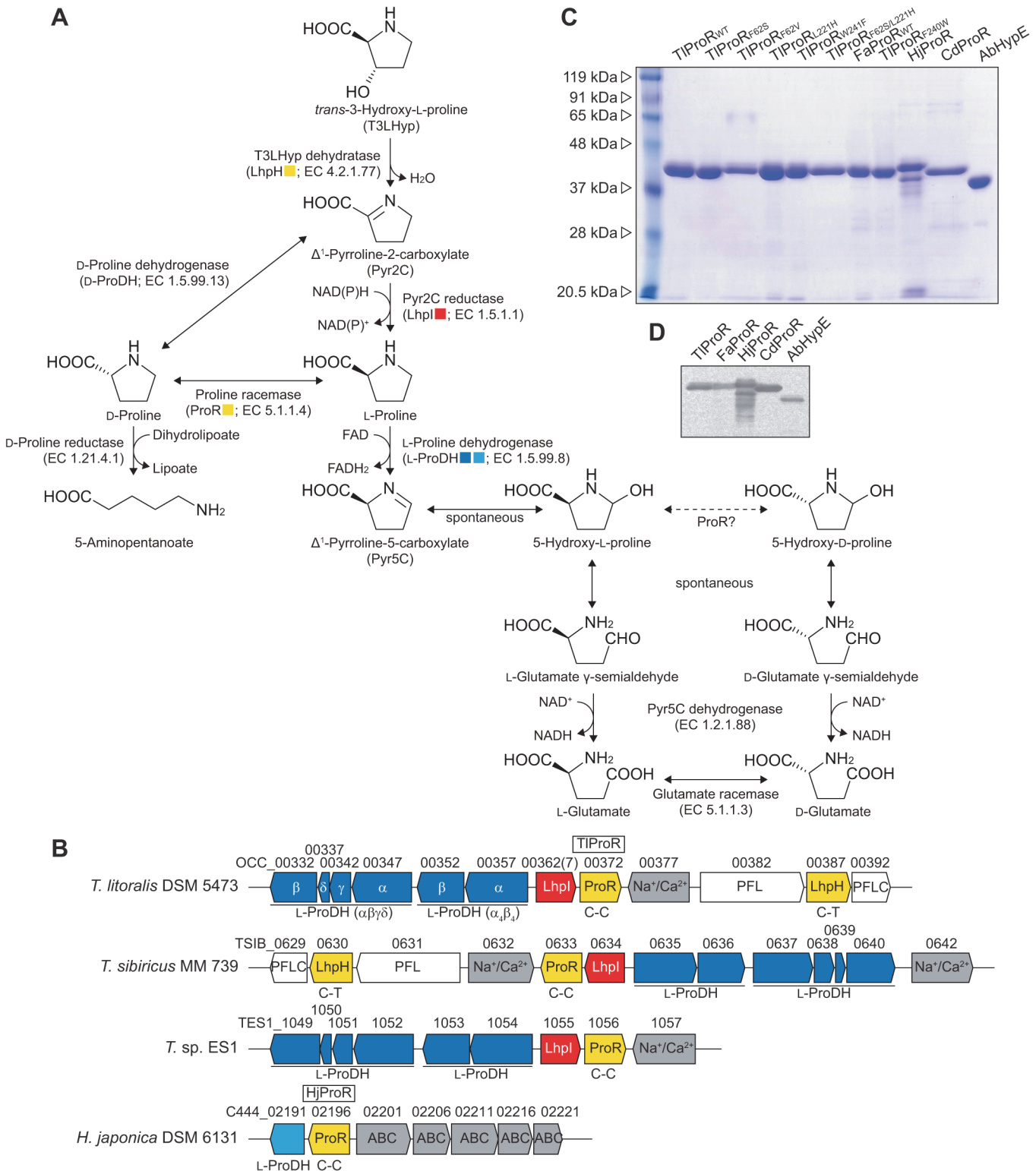


Fig 1. Putative metabolic network of proline and hydroxyproline in archaea. (A) Metabolic networks of L-proline, D-proline, and T3LHyp. (B) Genomic gene clusters related to the metabolism of proline and/or T3LHyp by archaea. Homologous genes are indicated in the same color and correspond to Fig 1A. Putative genes in the box were purified and characterized in this study (see Fig 1C). No clustering was found around the FaProR gene. C-C and C-T indicate a pair of catalytic amino acid residues of ProR superfamily enzymes. Gray putative genes are sequentially similar to other (amino acid) transporters. (C) Purification of recombinant His₆ tag proteins. Five micrograms each of the purified protein were applied to a 12% (w/v) gel. (D) Western blot analysis. One microgram each of the purified protein were applied to a 12% (w/v) gel.

doi:10.1371/journal.pone.0120349.g001

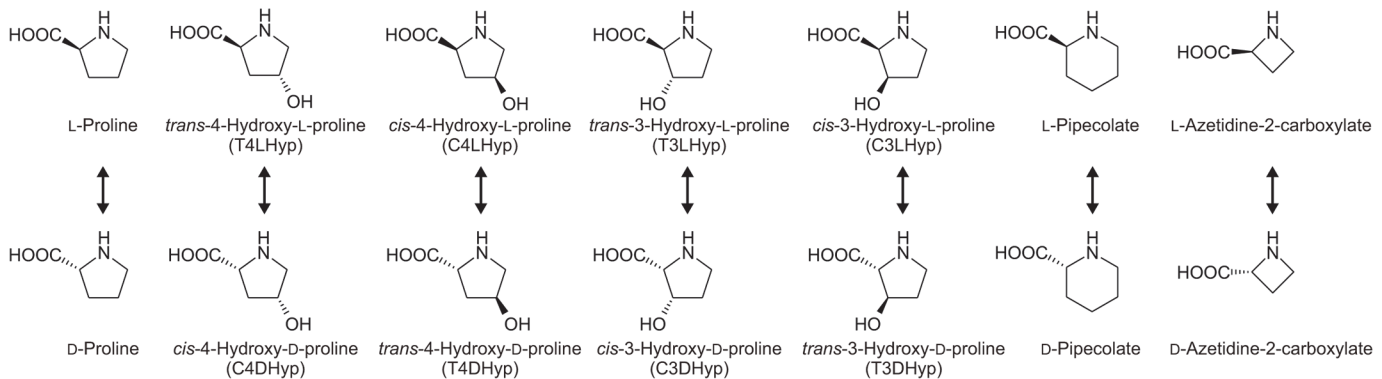


Fig 2. Library of proline derivatives. TIProR can enable the reversible racemization and epimerization of all proline derivatives (arrows).

doi:10.1371/journal.pone.0120349.g002

Following its spontaneous hydrolysis, the L-glutamate γ -semialdehyde produced is then oxidized to L-glutamate by Pyr5C dehydrogenase (EC 1.2.1.88). L-Proline is alternatively metabolized to 5-aminopentanoate through two enzymatic steps. L-Proline racemase (EC 5.1.1.4; ProR) first catalyzes the racemization of L-proline to D-proline, followed by reductive cleavage to yield 5-aminopentanoate by D-proline reductase (EC 1.2.1.4.1). This pathway is only operative in certain clostridia including *Clostridium sticklandii* [2] and *Clostridium difficile* [3], clinically significant nosocomial pathogens, and *Trypanosoma* species including *Trypanosoma cruzi* [4, 5] and *Trypanosoma vivax* [6], the causative agents of Chagas disease and animal trypanosomiasis, respectively. In the former, the pathway is involved in the so-called “Stickland reaction (fermentation)”, whereas ProR in the latter has been implicated in the mechanisms underlying the escape of parasites from host immunity as a B-cell mitogen.

Hydroxyproline has been detected in certain proteins, especially collagen, as well as some peptide antibiotics. In mammalian systems [1], the L-proline residue in procollagen is post-translationally hydroxylated to *trans*-4-hydroxy-L-proline (T4LHyp) or *trans*-3-hydroxy-L-proline (T3LHyp). Among the several stereoisomers of hydroxyproline including T4LHyp and T3LHyp (Fig. 2), T4LHyp is the most common in nature. In contrast to mammals [1], some bacteria have been shown to metabolize T4LHyp to α -ketoglutarate via three intermediates through four enzymatic steps [7, 8]. Of these, hydroxyproline 2-epimerase (HypE; EC 5.1.1.8) first catalyzes the isomerization of T4LHyp to *cis*-4-hydroxy-D-proline (C4DHyp), which is then converted to Δ^1 -pyrroline-4-hydroxy-2-carboxylate (Pyr4H2C) by C4DHyp dehydrogenase (D-HypDH). In the metabolism of T3LHyp (Fig. 1A), T3LHyp dehydratase (EC 4.2.1.77; T3LHypD) initially catalyzes the dehydration of T3LHyp to Δ^1 -pyrroline-2-carboxylate (Pyr2C) via a putative Δ^2 -pyrroline-2-carboxylate intermediate [9]. The Pyr2C is then converted by NAD(P)H-dependent Pyr2C reductase (EC 1.5.1.1) to yield L-proline, which is metabolized through the general degradation of L-proline described above. This pathway is most commonly found in mammals [9], bacteria [10] and archaea [11].

Racemase enzymes catalyze the deprotonation/reprotonation of the chiral carbon ($C\alpha$) of both amino acid enantiomers, resulting in the stereoinversion of chiral centers. ProR is a member of the pyridoxal 5'-phosphate (PLP)-independent racemase family along with HypE and T3LHypD (although the reaction involving the latter is not epimerization) [9, 12, 13]. These enzymes have been classified into three types based on the two specific residues at the active sites [9]: the Cys-Cys type (ProR and HypE), Cys-Thr type (T3LHypD), and Ser-Cys or Ser-Thr type (function unknown). In the cases of ProR and HypE, catalysis is based on the same 1,1-proton transfer mechanism using two general acidic/basic cysteine residues located on

opposite faces of the active site [12]. On the other hand, their substrate specificities were previously considered to be very strict: proline for ProR [13] and T4LHyp and *cis*-4-hydroxy-L-proline (C4LHyp) for HypE [13, 14]. Although the catalytic mechanism of T3LHypD currently remains unclear, dehydration may start by the abstraction of a proton from the C α of the substrate by an active site cysteine residue as a general basic catalyst [9]. This enzyme can also only utilize T3LHyp as a substrate.

As described above, no racemase/epimerase from the ProR superfamily had been found in archaea. We here identified and characterized a ProR-like protein with a pair of Cys-Cys as (putative) active sites from the hyperthermophilic marine archaeon, *Thermococcus litoralis* [15], which differed from the previously isolated T3LHypD enzyme [11]. This protein could reversibly catalyze not only the racemization of proline, but also the epimerization of 4-hydroxyproline and 3-hydroxyproline with similar kinetic constants. Site-directed mutagenesis revealed several important amino acid residue(s) responsible for discriminating between proline and hydroxyproline. A phylogenetic analysis indicated that such unique broad substrate specificity was derived from an ancestral enzyme of this superfamily. To the best of our knowledge, this is the first study on the bifunctional enzyme of ProR and HypE from archaea.

Materials and Methods

Materials

T3LHyp was purchased from Kanto Chemical (Tokyo, Japan). C4LHyp, L-pipecolate, and D-pipecolate were obtained from Tokyo Chemical Industry (Tokyo, Japan). T4DHyp and C3LHyp were from Sigma Aldrich (USA). T4LHyp, C4DHyp, L-proline, and D-proline were from Wako Pure Chemical Industries (Osaka, Japan).

General procedures

Basic recombinant DNA techniques were performed as described by Sambrook *et al.* [16]. Archaeal genomic DNA was prepared using a DNeasy Tissue Kit (Qiagen). PCR was carried out using a GeneAmp PCR System 2700 (Applied Biosystems) for 30 cycles in 50 μ l of reaction mixture containing 1 U of KOD FX DNA polymerase (TOYOBO), appropriate primers (15 pmol), and template DNA under the following conditions: denaturation at 98°C for 10 s, annealing at 50°C for 30 s, and extension at 68°C for time periods calculated at an extension rate of 1 kbp·min⁻¹. DNA sequencing was carried out using the BigDye Cycle Sequencing Kit ver.3.1 (Applied Biosystems) and appropriate primers with the Genetic Analyzer 3130 (Applied Biosystems). High-pressure liquid chromatography (HPLC) was performed using an Agilent 1120 Compact LC system (TOSOH). Protein concentrations were determined by the method of Lowry *et al.* [17] with bovine serum albumin as the standard. SDS-PAGE was performed as previously described by Laemmli [18]. Western blot analysis was carried out using an ECL Western Blotting Analysis System (GE Healthcare) and RGS-His HRP antibody (horse-radish peroxidase-fused mouse monoclonal antibody against Arg-Gly-Ser-His₆ in the N-terminal additional peptide of the expressed recombinant proteins (Qiagen))

Plasmid construction for expression of recombinant proteins

The primer sequences used in this study are shown in S1 Table. In this study, the prefixes Tl (*T. litoralis*), Fa (*Ferroplasma acidiphilum*), Hj (*Haloarcula japonica*), Cd (*C. difficile*), and Ab (*Azospirillum brasilense*) were added to gene symbols or protein designations where necessary for clarity. The *TlProR* (GenBank accession number OCC_00372), *FaProR* (FACI_I-FERC00001G0786), *HjProR* (C444_02196), *CdProR* (CD630_32370), and *AbHypE* genes

(BAN78527) were amplified by PCR using primers containing appropriate restriction enzyme sites at the 5'- and 3'-ends and the genomic DNA of *T. litoralis* DSM 5473, *F. acidiphilum* DSM 12658, *H. japonica* DSM 6131, *C. difficile* 630, or *A. brasilense* ATCC 29145 as a template, respectively. Each amplified DNA fragment was introduced into BamHI-SalI sites (for the *TlProR*, *FaProR*, and *CdProR* genes), BamHI-PstI (for the *HjProR* gene), or BamHI-HindIII (for the *AbHypE* gene) in pETDuet-1 (Novagen), a plasmid vector used to confer an N-terminal His₆ tag on expressed proteins, to obtain pET/*TlProR*_{WT}, pET/*FaProR*_{WT}, pET/*HjProR*, pET/*CdProR*, and pET/*AbHypE*_{WT}, respectively.

In the present study, we used *F. acidiphilum* DSM 12658 instead of *Ferroplasma acidarmanus* fer1 as a target microorganism, for which there was 99% identity in the 16S rRNA sequence. We successfully amplified the *FaProR* gene by genomic PCR using oligonucleotide primers designed from the *F. acidarmanus* fer1 genome sequence. Unless otherwise noted, *Ferroplasma* sp. hereafter indicates strain DSM 12658.

Expression and purification of His₆-tagged recombinant proteins

Escherichia coli BL21-CodonPlus(DE3)-RIL (Novagen) harboring the constructed pETDuet-1 plasmid was grown at 37°C to a turbidity of 0.6 at 600 nm in Super broth medium (pH 7.0, 12 g tryptone, 24 g yeast extract, 5 ml glycerol, 3.81 g KH₂PO₄, and 12.5 g K₂HPO₄ per liter) containing 50 mg/liter ampicillin. After the addition of 1 mM isopropyl-β-D-thiogalactopyranoside (IPTG), the culture was grown for a further 6 h to induce the expression of the His₆-tagged protein. The grown cells were harvested by centrifugation at 30,000 × g for 20 min, suspended in Buffer A (50 mM sodium phosphate buffer (pH 8.0) containing 300 mM NaCl and 10 mM imidazole), disrupted by sonication for 20 min at appropriate intervals on ice using Ultra Sonic Disruptor UD-211 (TOMY SEIKO Co., Ltd, Tokyo, Japan), and then centrifuged at 108,000 × g for 20 min at 4°C. The supernatant was loaded onto a Ni-NTA Superflow column (Qiagen) equilibrated with Buffer A linked to the BioAssist eZ system (TOSOH). The column was washed with Buffer B (50 mM sodium phosphate buffer (pH 8.0) containing 300 mM NaCl, 10% (v/v) glycerol, and 50 mM imidazole). The enzymes were then eluted with Buffer C (pH 8.0, Buffer B containing 250 mM imidazole instead of 50 mM imidazole), concentrated by ultrafiltration with Centriplus YM-30 (Millipore), dialyzed against 50 mM Tris-HCl buffer (pH 8.0) containing 50% (v/v) glycerol, and stored at -35°C until use.

The native molecular mass of recombinant proteins was estimated by gel filtration, which was carried out using a HPLC system at a flow rate of 1 ml/min. The purified enzyme was loaded onto a TSKgel G3000SWXL column (TOSOH) equilibrated with 50 mM Tris-HCl buffer (pH 8.0). A high molecular weight gel filtration calibration kit (GE Healthcare) was used for molecular markers.

Enzyme assay by HPLC

Purified protein was added to 50 mM Tris-HCl buffer (pH 8.0) (1 ml) containing 10 mM substrate, and incubated at 50°C (for *TlProR* and *HjProR*) or 30°C (*FaProR*, *CdProR*, and *AbHypE*). After varying the incubation times, the enzyme reaction was stopped by rapidly incubating at -80°C. To this solution, 25 μl each of 10 mM 4-fluoro-7-nitrobenzofurazan (NBD-F) in ethanol and 100 mM borate buffer (pH 8.0) was then added and incubated at 60°C for 1 min. A total of 1.15 ml of 5 mM HCl was finally added to the reaction mixture, followed by filtration through a 0.22-μm filter (Millipore). HPLC analysis was carried out using an Ultron ES-CD chiral separation column (150 × 2.0 mm, Shinwa Chemical Industries). The flow rate was 1 ml·min⁻¹, and isocratic elution with 20 mM potassium phosphate (pH 6.0) containing 10% (v/v) methanol was monitored by absorbance at 530 nm. Non-enzymatic

conversion of L \leftrightarrow D isomers was observed even after being incubated for 12 h, and the difference in background turnover between 30°C and 50°C was negligible. This method was used to estimate the effects of substrate specificity and inhibition by pyrrole-2-carboxylate (PYC) on activity.

Spectrophotometric enzyme assay

Racemase/epimerase activity for proline or hydroxyproline(s) was spectrophotometrically assayed at 50°C by monitoring the reduction rate of an artificial electron acceptor in the coupling system with dehydrogenase for proline or hydroxyproline, using a Shimadzu UV-1800 spectrophotometer (Shimadzu GLC Ltd., Tokyo, Japan).

Activity toward L-proline and T3LHyp. The standard reaction mixture contained 0.05 mM 2,6-dichloroindophenol (Cl2Ind) and purified D-ProDH from *Pyrobaculum islandicum* (20 μ g) [19] in 50 mM Tris-HCl buffer (pH 8.0).

Activity toward D-proline. The standard reaction mixture contained 0.05 mM Cl2Ind and purified L-ProDH from *Aeropyrum pernix* (20 μ g) [20] in 50 mM Tris-HCl buffer (pH 8.0).

Activity toward T4LHyp. The standard reaction mixture contained 0.25 mM *p*-iodonitrotriazolium violet (INT), 0.06 mM phenazine methosulfate (PMS), and purified D-HypDH from *A. brasiliense* (20 μ g) [21] in 50 mM Tris-HCl buffer (pH 8.0).

All reactions were initiated by the addition of 100 mM substrate (100 μ l) with a final reaction volume of 1 ml. The millimolar absorption coefficients (ϵ) for Cl2Ind and INT were 19.1 mM⁻¹·cm⁻¹ at 600 nm and 15.0 mM⁻¹·cm⁻¹ at 490 nm, respectively. The detectable limit of specific activity was \sim 0.001 unit/mg protein, due to non-enzymatic absorbance change by Cl2Ind and PMS/INT. This method was used to determine the kinetic parameters, K_m and k_{cat} , which were calculated by a Lineweaver-Burk plot.

Identification of reaction products

To remove glycerol in the stored buffer, purified TlProR (10 μ g) was dialyzed at 4°C overnight in 50 mM potassium phosphate buffer (pH 7.0), lyophilized, and solved in D₂O (600 μ l) containing 20 mM T4LHyp or T3LHyp. NMR spectra were recorded at 25°C on a JEOL JNM-EC400 NMR spectrometer (JEOL Ltd., Tokyo, Japan) operating at 400 MHz. 2,2-Dimethyl-2-silapentane-5-sulfonate was used as an internal standard. ¹H NMR spectra of T4LHyp and T3LHyp (400 MHz, D₂O) were as follows: T4LHyp, 4.41 (1H, t, $J = 4$ Hz), 4.33 (1H, dd, $J_1 = 10$ Hz, $J_2 = 8$ Hz), 3.47 (1H, dd, $J_1 = 12$ Hz, $J_2 = 4$ Hz), 3.35 (1H, ddd, $J_1 = 12$ Hz, $J_2 = J_3 = 2$ Hz), 2.42 (1H, dddd, $J_1 = 14$ Hz, $J_2 = 8$ Hz, $J_3 = J_4 = 2$ Hz), and 2.15 (1H, ddd, $J_1 = 14$ Hz, $J_2 = 10$ Hz, $J_3 = 4$ Hz); C4DHyp, 4.57 (1H, m), 4.21 (1H, dd, $J_1 = 11$ Hz, $J_2 = 4$ Hz), 3.36 (1H, dd, $J_1 = 12$ Hz, $J_2 = 4$ Hz), 2.50 (1H, ddd, $J_1 = 14$ Hz, $J_2 = 10$ Hz, $J_3 = 4$ Hz), and 2.25 (1H, m); T3LHyp, 4.68 (1H, m), 4.07 (1H, s), 3.60 (1H, m), 3.50 (1H, m), and 2.04 (2H, m); C3DHyp, 4.71 (1H, m), 4.14 (1H, d, $J = 4$ Hz), 3.56 (1H, m), 3.48 (1H, m), and 2.18 (2H, m).

Site-directed mutagenesis

A mutation was introduced into the *TlProR*, *FaProR*, or *AbHypE* genes by sequential steps of PCR [22] using sense and antisense primers (S1 Table) and pET/TlProR_{WT} (for TlProR_{F62S} (CTG \rightarrow AGG), TlProR_{F62V} (CTG \rightarrow GTT), TlProR_{L221H} (CTG \rightarrow GAG), TlProR_{F62S/L221H}, TlProR_{W241F} (GTG \rightarrow GAC), TlProR_{W241C} (CTG \rightarrow TGT), and TlProR_{W241Y} mutants (CTG \rightarrow TAT)), pET/FaProR_{WT} (for FaProR_{F240W} mutant (GCC \rightarrow AAG)), or pET/AbHypE_{WT} (for AbHypE_{C226F} mutant (GTG \rightarrow TTC)) as a template (the codons used for each mutation were in parentheses). The coding region of the mutated genes was confirmed by

subsequent sequencing in both directions. Mutant proteins were expressed and purified by the same procedures as those for the wild-type enzyme.

Amino acid sequence alignment and phylogenetic analysis

Protein sequences were analyzed using the Protein-BLAST and Clustal W program distributed by DDBJ (DNA Data Bank of Japan) (www.ddbj.nig.ac.jp). The phylogenetic tree was produced using the TreeView 1.6.1. program.

Results

Putative ProR or HypE, but not the T3LHypD gene from archaea

We previously reported that OCC_00387 and OCC_00362(7) from *T. litoralis* encoded T3LHypD and Pyr2C reductase are involved in (putative) T3LHyp metabolism, respectively [11] (Fig. 1A). These genes were clustered on the genome together with several other hypothetical genes (Fig. 1B), among which OCC_00357 (α -subunit) and OCC_00352 (β) (genes) were homologous to $\alpha_4\beta_4$ -type L-ProDH from *Pyrococcus horikishii* (PH1363 and PH1364 with 69 and 80% identities, respectively) [23], while OCC_00347 (α), OCC_00342 (γ), OCC_00337 (δ), and OCC_00332 (β) (genes) were similar to $\alpha\beta\gamma\delta$ -type L-ProDH from *Thermococcus profundus* (pdhA, pdhF, pdhX, and pdhB with 81, 72, 72, and 64% identities, respectively) [24]. Since T3Lhyp is metabolized to L-proline via a Pyr2C intermediate [9–11], the gene cluster may be related to both the (general) metabolism of L-proline and T3LHyp. Another ProR-like gene (OCC_00372) was also detected in this gene cluster, and the putative amino acid sequence contained two cysteine residues at the active sites (Cys⁸⁸-Cys²⁵¹) specific for ProR or HypE, but not T3LHypD (see below). Furthermore, by a homology search using the Protein-BLAST program, some archaea including *F. acidarmanus* (*F. acidiphilum*) and *H. japonica* were found to possess the homologous gene (see below in detail). Therefore, in the present study, we selected three ProR-like genes from *T. litoralis*, *F. acidiphilum*, and *H. japonica* as target genes (referred to as TlProR, FaProR, and HjProR genes, respectively). Furthermore, ProR from *C. difficile* [13] and HypE from *A. brasilense* [21] were used as controls (referred to as CdProR and AbHypE, respectively).

Preparation of recombinant His₆-tag proteins

After cloning all target genes into the vector pETDuet-1, the recombinant enzymes were successfully expressed in *E. coli* cells as His₆-tagged enzymes, and purified to homogeneity using a nickel-chelating affinity column (Fig. 1C). Additional amino acid residues including the His₆-tag at the N-terminal was confirmed by western blot analysis with an anti-His₆-tag antibody (Fig. 1D). The apparent molecular masses of TlProR, FaProR, HjProR, CdProR, and AbHypE, as estimated by SDS-PAGE, were 40 (38.1), 40 (38.5), 42 (35.8), 40 (37.7) and 37 (34.1) kDa (values in parentheses indicate the calculated molecular mass of the enzyme with His₆-tag), while those estimated by analytic gel filtration were ~80 kDa, respectively (data not shown). Therefore, all these enzymes appeared to be dimeric.

Substrate specificity of TlProR

Stereoisomer identification and quantification by potential enzyme reactions were determined by chiral separation column chromatography, in which a sample was derivatized with NBD-F. The typical retention times (min) of the tested substrates (Fig. 2) were follows: L-proline, 12.9; D-proline, 11.6; T4LHyp, 8.2; C4DHyp, 8.7; C4LHyp, 9.5; T4DHyp, 7.1; T3LHyp, 8.0;

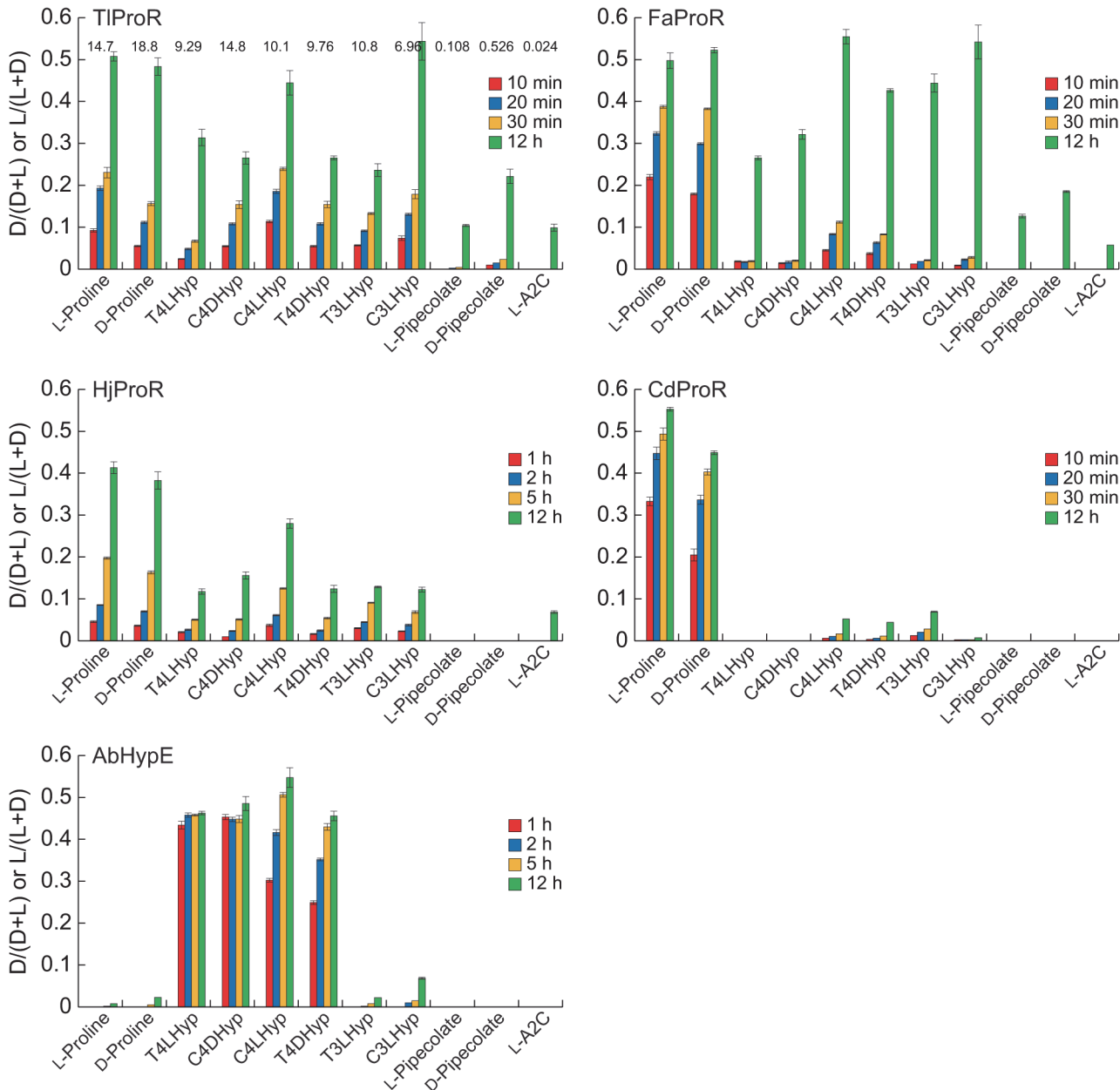


Fig 3. Substrate specificities of TIProR, FaProR, HJProR, CdProR, and AbHypE. The reaction mixture (1 ml) consisted of 10 mM of substrate and each purified enzyme as follows in Tris-HCl buffer (pH 8.0): TIProR, 1.3 µg; FaProR, 100 µg; HJProR, 570 µg; CdProR, 3.6 µg; AbHypE, 4.9 µg. L-A2C is L-azetidine-2-carboxylate. Samples at the indicated times were analyzed by HPLC (means ± S.D., n = 3). Values on the bars of TIProR indicate specific activity (unit/mg protein), which are similar to those in Tables 1 and 2.

doi:10.1371/journal.pone.0120349.g003

(putative) C3DHyp, 8.5; C3LHyp, 9.8; (putative) T3DHyp, 7.3; L-pipecolate, 15.4; D-pipecolate, 14.7; L-azetidine-2-carboxylate, 9.1; (putative) D-azetidine-2-carboxylate, 8.6.

TIProR could catalyze the conversion of not only L-proline, but also 4-hydroxy-L-proline (T4LHyp (63) and C4LHyp (69)) and 3-hydroxy-L-proline (T3LHyp (73) and C3LHyp (47)) (values in parentheses indicate specific activity as a percentage of L-proline) (Fig. 3). The reaction was completely bi-directional, and the reverse reactions were also similar: D-proline (130), C4DHyp (160), and T4DHyp (97) (values in parentheses indicate specific activity as a

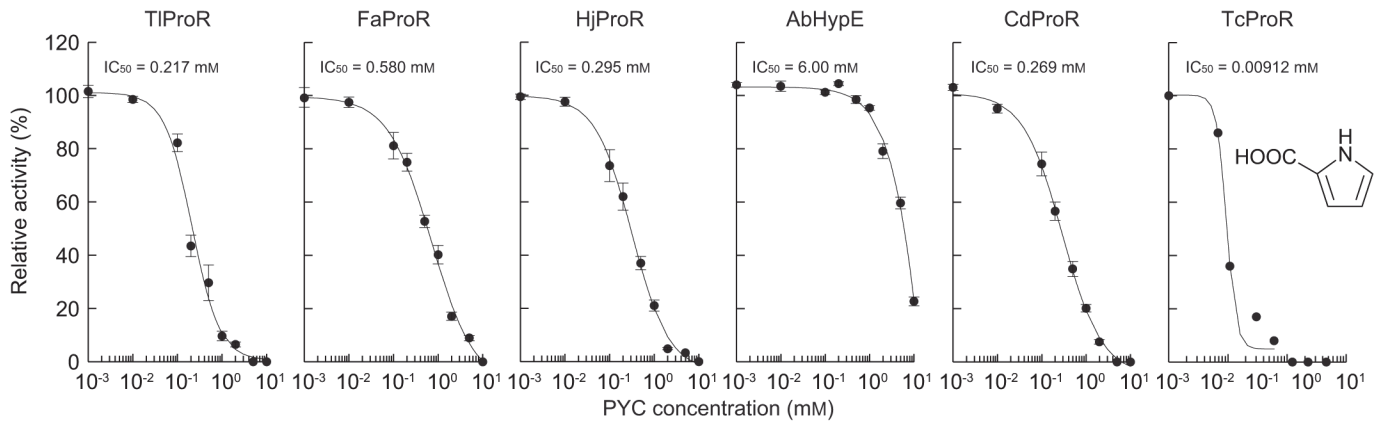


Fig 4. Unique inhibition of archaeal ProR-like enzymes by pyrrole-2-carboxylate (PYC; inset). Reactions were performed for 30 min with the same conditions as those in Fig. 3, except for the presence of several concentration of PYC. L-Proline (for TIPrOR, FaPrOR, HjPrOR, and CdPrOR) or T4LHyp (for AbHypE) was used as a substrate. Relative specific activity values were expressed as percentages of the values obtained in the absence of PYC (means \pm S.D., $n = 3$). Data for the ProR of *T. cruzi* (TcPrOR) are from Berneman et al. [25]. IC_{50} values were calculated by curve fitting using ImageJ software (<http://rsb.info.nih.gov/ij/>).

doi:10.1371/journal.pone.0120349.g004

percentage of L-enantiomer). Furthermore, using large amounts of the purified enzyme, we could also estimate specific activities for L-pipecolate (0.7), D-pipecolate (3.6), and L-azetidine-2-carboxylate (0.16), which are the six- and four-membered ring analogs of proline, respectively.

Another previously reported difference in the properties of ProR and HypE is the profile of inhibition by pyrrole-2-carboxylate (PYC), a transition state analogue of proline [6, 13, 25]: ProR enzymes from trypanosomatids and clostridia were inhibited at even 0.01 and 1 mM, respectively, whereas HypE reactions were only affected by high amounts of PYC (~ 10 mM), as described in CdPrOR and AbHypE (Fig. 4). In spite of the significant HypE activity, the IC_{50} value of TIPrOR (0.217 mM) was ~ 28 -fold higher than that of AbHypE (6.00 mM), confirming dual activity toward proline and 4-hydroxyproline.

Kinetic analysis of TIPrOR

A more sensitive spectrophotometric assay method using proline or hydroxyproline dehydrogenase as a coupling enzyme was developed to estimate kinetic properties. The kinetic parameters of proline and hydroxyproline determined from the Lineweaver-Burk plot are shown in Tables 1 (L \rightarrow D) and 2 (D \rightarrow L). The catalytic efficiency (k_{cat}/K_m) values for L-proline and T4LHyp were similar, whereas a preference for D-proline over C4DHyp (45-fold) was identified and was caused by a 75-fold lower K_m for D-proline. This may have been partially due to differences in the K_m values of L-ProDH (0.28 mM) [20] and D-ProDH (4.2 mM) [19] as the coupling enzyme used. TIPrOR was assayed at 50°C, which was far from the optimum temperature (90 \sim 100°C; data not shown). Although the k_{cat}/K_m value for T4LHyp of TIPrOR was 27-fold lower than that for AbHypE, the specific activity of the former at 100°C, estimated by HPLC analysis, was similar to that of the latter: 29.1 and 58.6 unit/mg protein, respectively.

Zhao et al. [26] recently characterized 51 ProR-like proteins from bacteria. Of these, the k_{cat}/K_m value for T4LHyp of HypE from *Pseudomonas putida* was 192 and 3430-fold higher than those for T3LHyp and L-proline, respectively, and was caused by a markedly higher k_{cat} value. Similar results were also obtained for other (putative) HypE proteins. In contrast, the kinetic constant for T3LHyp of TIPrOR was similar to those of L-proline and T4LHyp. Thus, to

the best of our knowledge, this is the first example of a ProR-like protein being capable of utilizing not only proline, but also 4-hydroxyproline and 3-hydroxyproline as a substrate.

Identification of reaction products by TIProR

T4LHyp was incubated with TIProR in D₂O at various incubation times. ¹H NMR spectra showed the progressive loss of H₁ peaks, and additionally contained resonances associated with C4DHyp, a potential product: an exchange of the α-proton with solvent deuterium (Fig. 5A). Similar phenomena were also observed when T3LHyp was used as a substrate instead of T4LHyp (Fig. 5B). These results were expected for a 1,1-proton transfer reaction that equilibrates the configurations at Cα of not only 4-hydroxyproline, but also 3-hydroxyproline (novel activity), as proposed previously [12].

Phylogenetic analysis of TIProR

As expected from the preliminary annotation, TIProR belongs to the ProR superfamily, which consists of four subfamilies: the archetype ProR (blue in Fig. 6), HypE (light green), T3LHypD (orange), and function unknown protein (yellow). Only two putative proteins from the

Table 1. Kinetic parameters for L-proline, T4LHyp, and T3LHyp.

Enzymes	Substrates	Specific activity ^a (units/mg protein)	K _m (mM)	k _{cat} (min ⁻¹)	k _{cat} /K _m (min ⁻¹ ·mM ⁻¹)	ProR HypE
TIProR _{WT}	L-Proline	3.45	1.21±0.12	167±10	138±4	—
	T4LHyp	9.69	6.08±1.76	728±146	122±13	1.1 ^b
	T3LHyp	3.67	0.502±0.021	216±4	430±10	0.32
TIProR _{W241F}	L-Proline	5.19	1.29±0.14	190±14	147±5	—
	T4LHyp	2.13	4.28±0.84	92.0±10.5	21.7±1.7	6.8
	T3LHyp	0.160	16.4±3.2	17.5±2.5	1.07±0.07	137
TIProR _{L221H}	L-Proline	0.488	20.5±2.5	55.4±6.1	2.71±0.05	0.45
	T4LHyp	0.670	6.50±0.39	39.0±1.7	6.01±0.11	—
TIProR _{F62S}	L-Proline	0.0195	154±13	12.0±1.1	0.0774±0.0010	0.20
	T4LHyp	0.0384	6.22±0.62	2.35±0.17	0.379±0.012	—
TIProR _{F62V}	L-Proline	0.0691	1.93±0.44	5.51±0.99	2.88±0.15	0.33
	T4LHyp	0.0972	0.905±0.075	7.84±0.49	8.67±0.18	—
TIProR _{F62S/L221H}	L-Proline	0.001>	N.D. ^c	N.D.	N.D.	—
	T4LHyp	0.001>	N.D.	N.D.	N.D.	—
FaProR _{WT}	L-Proline	0.29	31.6±5.3	35.8±5.6	1.13±0.01	2.9
	T4LHyp	0.0209	6.12±0.30	2.37±0.10	0.387±0.002	—
FaProR _{F240W}	L-Proline	0.117	53.0±8.0	25.0±3.4	0.473±0.008	1.4
	T4LHyp	0.00822	2.17±0.13	0.717±0.032	0.331±0.005	—
CdProR	L-Proline	14.2	8.53±0.47	849±27	99.6±57	—
	T4LHyp	0.0975	N.D.	N.D.	N.D.	—
AbHypE _{WT}	L-Proline	0.124	N.D.	N.D.	N.D.	—
	T4LHyp	58.6	1.39±0.15	4400±340	3180±100	—
AbHypE _{C226F}	L-Proline	0.001>	N.D.	N.D.	N.D.	—
	T4LHyp	0.001>	N.D.	N.D.	N.D.	—

^aUnder standard assay conditions in the “Materials and Methods”.

^bRatio of L-proline to T4LHyp or T3LHyp in k_{cat}/K_m.

^cNot determined due to trace activity.

doi:10.1371/journal.pone.0120349.t001

Table 2. Kinetic parameters for D-proline and C4DHyp.

Enzymes	Substrates	Specific activity ^a (units/mg protein)	K_m (mM)	k_{cat} (min ⁻¹)	k_{cat}/K_m (min ⁻¹ ·mM ⁻¹)	ProR HypE
TIProR _{WT}	D-Proline	3.45	0.0919±0.006	133±2	1570±90	45.1 ^b
	C4DHyp	3.48	6.65±0.69	230±12	34.8±1.8	
TIProR _{W241F}	D-Proline	4.87	0.194±0.020	191±5	990±82	158
	C4DHyp	0.681	6.70±0.68	41.8±2.7	6.25±0.24	
TIProR _{L221H}	D-Proline	0.299	2.54±0.46	17.3±2.7	6.84±0.19	4.3
	C4DHyp	0.111	4.18±0.81	6.66±1.31	1.59±0.00	
TIProR _{F62S}	D-Proline	0.0283	4.00±0.17	1.55±0.09	0.387±0.008	1.4
	C4DHyp	0.0186	3.14±0.15	0.859±0.012	0.274±0.010	
TIProR _{F62V}	D-Proline	0.0309	0.156±0.004	1.41±0.03	9.04±0.23	–
	C4DHyp	0.00661	N.D.	N.D.	N.D.	
TIProR _{F62S/L221H}	D-Proline	>0.001	N.D.	N.D.	N.D.	–
	C4DHyp	>0.001	N.D.	N.D.	N.D.	
FaProR _{WT}	D-Proline	0.164	1.17±0.09	7.09±0.12	6.09±0.35	–
	C4DHyp	0.00234	N.D. ^c	N.D.	N.D.	
FaProR _{F240W}	D-Proline	0.141	3.12±0.08	7.21±0.06	2.31±0.04	–
	C4DHyp	0.00230	N.D.	N.D.	N.D.	
CdProR	D-Proline	3.92	0.612±0.158	149±34	245±8	–
	C4DHyp	>0.001	N.D.	N.D.	N.D.	

^aUnder standard assay conditions in the “Materials and Methods”.

^bRatio of D-proline to C4DHyp in k_{cat}/K_m .

^cNot determined due to trace activity.

doi:10.1371/journal.pone.0120349.t002

hyperthermophilic archaeon *Thermococcus sibiricus* (TSIB_0633) and *Thermococcus* sp. ES1 (TES1_1056) showed >85% sequential identity (referred to as TIProR subfamily; red), and the corresponding genes formed a similar gene cluster to *T. litoralis*, together with (putative) L-ProDH and Pyr2C reductase genes (Fig. 1B). Although TIProR (subfamily) is not strongly related to any of the subclasses of the other members (30 ~ 40% sequence identity), a Protein-BLAST analysis revealed that TIProR was a close, but distinct subfamily of the ProR subfamily; the (putative) ligand binding sites were similar to those of ProR, but not HypE or T3LHypD, as described below. Furthermore, we found that two putative proteins (Cys-Cys type) from the hyperacidophilic archaeon *F. acidarmanus* (FaProR) and *Ferroplasma* sp. type II were located between the TIProR and ProR subfamilies (purple in Fig. 6). Several halophilic archaea including *H. japonica* (HjProR) (pink) also possessed similar types of proteins (genes), but formed a distinct subfamily to any other subfamily, and were often clustered with putative bacterial type (but not archaeal) L-ProDH (PutA) (Fig. 1B).

Characterization of FaProR and HjProR

To further estimate the evolutionary insight of archaeal ProR-like protein(s), FaProR and HjProR were characterized enzymatically using purified recombinant proteins (Fig. 1C). The racemization activity of proline was found to be significant in FaProR, although specific activity was ~10-fold lower than that of TIProR (Fig. 3). On the other hand, the k_{cat}/K_m value for T4LHyp was ~3-fold lower than that for L-proline, which was attributed to a 17-fold lower k_{cat} value, and we could not determine the kinetic parameters of the epimerization of C4DHyp

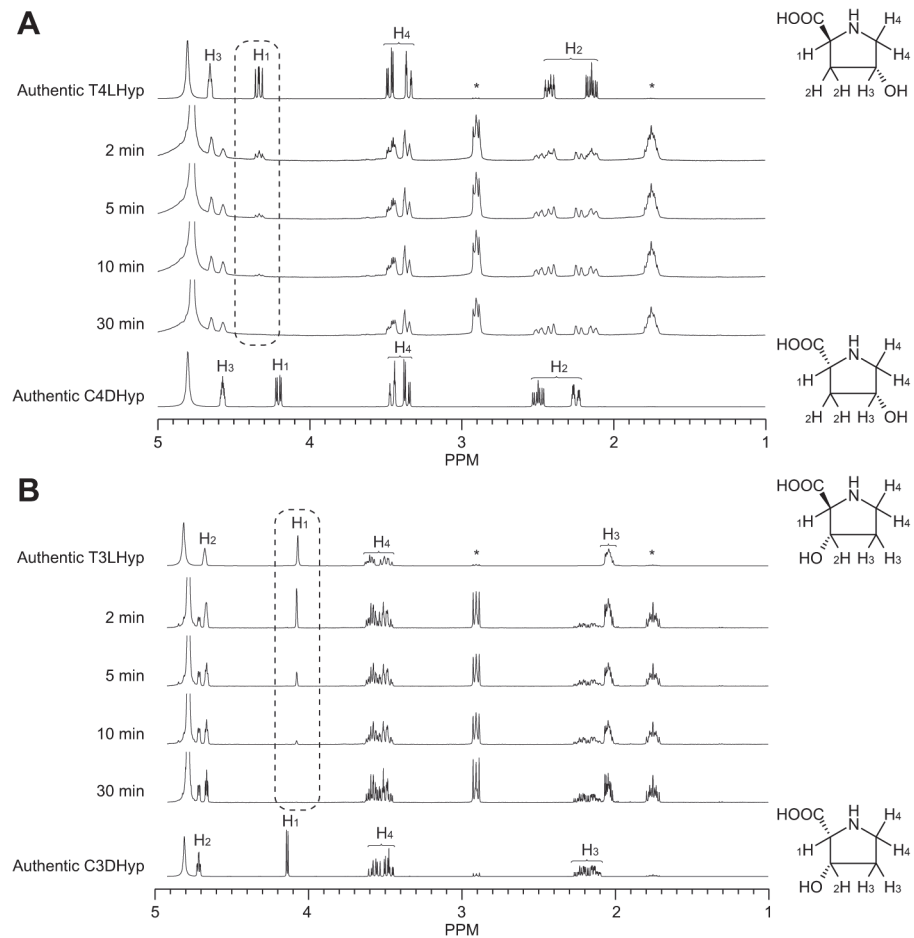


Fig 5. Representative ¹H NMR spectra for epimerase activity toward T4LHyp (A) and T3LHyp (B) by TlProR. Asterisks are peaks derived from an internal standard. Left panels show the assignments of protons in D₂O. The dashed line box indicates the progressive loss of H₁ peaks.

doi:10.1371/journal.pone.0120349.g005

to T4DHyp due to this low activity (Tables 1 and 2). Although similar results were obtained from the HPLC analysis (Fig. 3), L- or D-hydroxyproline(s) was significantly converted to another enantiomer(s) after being incubated for 12 h. These results suggested that the substrate specificity of FaProR was more similar to the known ProR enzymes than that of TlProR, confirming a phylogenetic relationship, as described above.

Although HjProR could also catalyze proline racemization, (low) specific activity was unmeasurable possibly due to the partial proteolysis (Fig. 1CD) and/or the enzyme from extreme halophilus: activation by salts is frequently necessary for full activity recovery [27]. Therefore, substrate specificity was preliminarily estimated by HPLC analysis using samples that had been incubated for 12 h (Fig. 3), and the enzyme could utilize both proline and hydroxyproline(s) as a substrate, similar to TlProR.

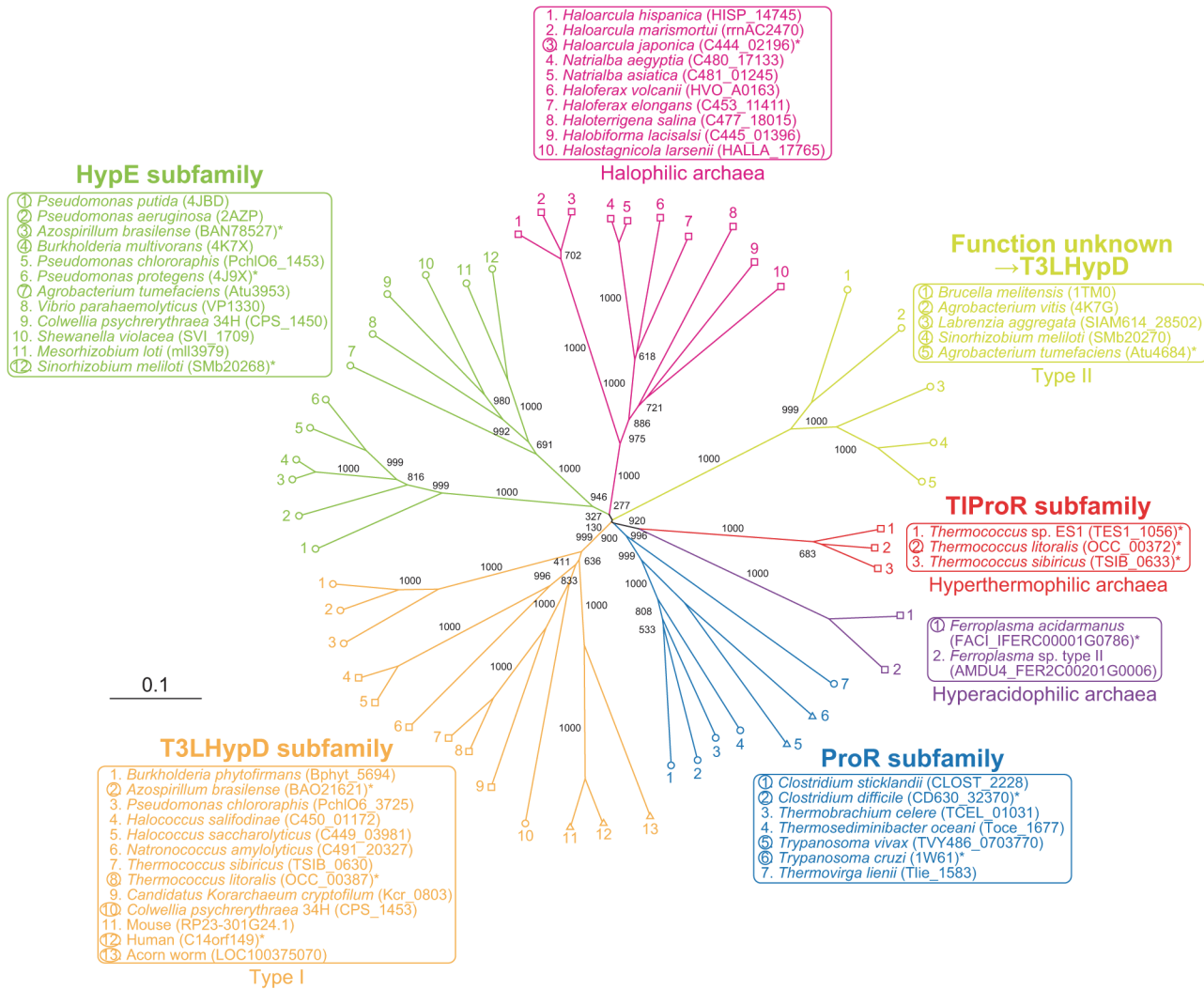


Fig 6. Phylogenetic tree of the ProR superfamily. The number on each branch indicates the bootstrap value. The circles, squares, and triangles at the end of each branch are enzymes from bacteria, archaea, and eukaryotes, respectively. Proteins with asterisks were used for Fig. 7. Proteins in circles were functionally characterized.

doi:10.1371/journal.pone.0120349.g006

Identification of amino acid residue(s) for discriminating between proline and hydroxyproline

In the crystal structure of the enzyme-T4LHyp complex of HypE from *Pseudomonas protegens* (PDB ID 4J9X) (33% identity with TIProR) [26], seven amino acid residues were detected close to the ligands, except for two catalytic cysteine residues (referred to as sites 1 ~ 7) (Fig. 7). Among them, sites 3, 6, and 7 were previously reported to be contained in two conserved motifs for the ProR superfamily (Met⁸⁷-Cys-Gly-His⁹⁰ and Asp²⁴⁷-Arg-Ser-Pro-Cys-Gly-Thr-Gly²⁵⁴; the numbers for TIProR), and formed hydrogen bonds with the carboxyl group or pyrrolidine nitrogen atom (shaded in green) [13].

TIProR possessed a tryptophan residue (Trp²⁴¹) at site 5 (shaded in pink), which was substituted to phenylalanine or cysteine/tyrosine in all known ProR (and also FaProR and HjProR) and HypE enzymes, respectively. Therefore, we constructed TIProR_{W241F}, TIProR_{W241C},

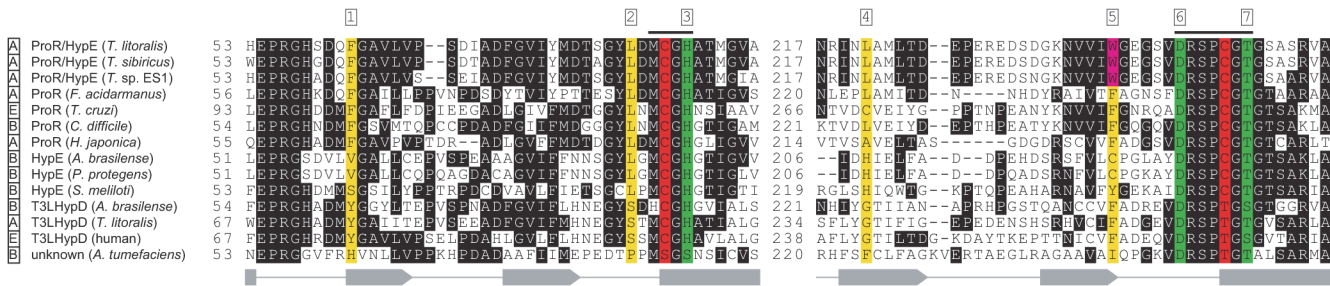


Fig 7. Partial multiple sequence alignment of deduced amino acid sequences of TIPrOR. A, B, and E are enzymes from archaea, bacteria, and eukaryotes, respectively. Consensus segments of the ProR superfamily are shown as a line on the sequence. Catalytic cysteine and/or threonine residues are shaded in red. Gray-shaded letters indicate highly conserved amino acid residues. Seven substrate binding sites are shaded in yellow and green, and the former interact with the carboxyl group or pyrrolidine nitrogen atom. The tryptophan residue, which is important for the discrimination of substrates (Trp²⁴¹ in TIPrOR), is shaded in pink. Gray-shaded letters indicate highly conserved amino acid residues. The secondary structures of ProR from *T. cruzi* (PDB ID 1W61), α -helix (rectangles) and β -sheets (arrows), are shown under the sequence.

doi:10.1371/journal.pone.0120349.g007

TlProR_{W241Y}, FaProR_{F241W}, and AbHypE_{C226F} mutants at an equivalent position. Of these, only the TlProR_{W241F}, FaProR_{F240W}, and AbHypE_{C226F} mutants successfully expressed in *E. coli* cells, as well as the wild-type (WT) enzyme (Fig. 1C). TlProR_{W241F} showed 5.3, 430, and 5.8-fold lower k_{cat}/K_m values for T4LHyp, T3LHyp, and C4DHyp respectively, mainly due to a marked decrease in k_{cat} values, whereas no significant effects were found in the kinetic constants of proline (Tables 1 and 2). FaProR_{F241W} showed similar kinetic constants for proline and hydroxyproline to the WT enzyme. The AbHypE_{C226F} mutant could utilize neither proline nor hydroxyproline(s) as a substrate. These results clearly indicated that tryptophan in the TlProR residue played important role(s) in both substrate specificity and structural folding, and favorably interacted with both the 4 and 3-hydroxy groups of hydroxyproline.

Phenylalanine at site 1 for ligand binding may only exist in ProR(-like) enzymes including TlProR, while histidine at site 4 could be specific for HypE. The three constructed TlProR mutants, F62S, F62V, and L221H, which mimic the natural HypE enzyme, moderately shifted substrate specificity toward 4-hydroxyproline (in particular, direction of L→D), and this was mainly attributed to a marked decrease in k_{cat} values; however, the prominent loss of both ProR and HypE catalysis was also observed, and there was no synergistic effect in a double mutant, F62S/L221H (Tables 1 and 2).

Discussion

The most interesting finding of the present study was the manner by which TlProR recognized both proline and 4-hydroxyproline (and 3-hydroxyproline) as substrates. Goytia et al. [13] proposed that several amino acid residues were responsible for this discrimination, in which two aromatic phenylalanine residues of ProR (at sites 1 and 5 in Fig. 7) may play the most important role(s) through hydrophobic interaction(s) between the enzyme and pyrrolidine ring of proline. If this hypothesis is correct, a mutation at the corresponding sites in ProR or HypE could significantly change each substrate specificity. However, when these amino acid residues are exchanged between ProR and HypE, the resultant mutant(s) can generally utilize neither proline nor hydroxyproline as a substrate: V60F for HypE from *Pseudomonas aeruginosa* [13], F62S and F62V for TlProR (this study), and C226F for AbHypE (this study). On the other hand, there is no doubt that TlProR (directly) evolved from an ancestor with phenylalanine at site 5 such as FaProR (Fig. 6). In other words, the W241F mutation (but not W241C and W241Y) mimicked the natural evolutionary process, through which no radical loss of activity occurred.

FaProR possessed the same ligand binding sites as natural ProR (Fig. 7). Therefore, it is unexpected that the (hydrophobic and bulky) tryptophan at site 5 of TlProR played an important role in the activity of hydroxyproline, which is more hydrophilic and bulkier than proline. No equivalent tryptophan was detected in the other members of the ProR superfamily, and many HypE enzymes including *Sinorhizobium meliloti* [28] possessed (the same aromatic and hydrophilic) tyrosine residue at that position, strongly suggesting that substrate specificity had been convergently acquired between TlProR and (natural) HypE. On the other hand, the environment in the active site pocket of TlProR seems to be suitable for recognizing hydroxyproline as a substrate independently of the amino acid residue at site 5, because FaProR, which possesses phenylalanine, but not tryptophan, at this position, as well as TlProR, shows similar IC_{50} value for inhibition by PYC to TlProR (Fig. 4). Several bacterial ProR-like proteins of the Ser-Thr type at the (putative) active sites (see in “Introduction”) have recently been functionally annotated as T3LHypD (Type II in Fig. 6) [26]. The ligand binding sites (1, 2, 4, and 5) were completely different from those of known T3LHypD (Type I) (Fig. 7). These results indicate that convergent evolution frequently occurred in the ProR superfamily, and also that there was more than one pattern for favorable binding of the same substrate. A previous study proposed that the last universal common ancestor (well denoted “LUCA” or “LCA”) was a hyperthermophilic organism [29] such as *T. litoralis* (98°C of maximum temperature for the growth) [15], and also that they possessed enzymes with significant broad substrate specificity [30]; therefore, the unique properties of TlProR may be (partially) derived from an ancient protein of the ProR superfamily.

The physiological role of TlProR has not yet been established. Since *T. litoralis* possesses no homologous gene to D-proline reductase, the physiological function of TlProR may be to epimerize hydroxyproline, but not racemize proline, confirming the evolutionary scenario proposed above. *T. litoralis* significantly accumulated T4LHyp as an intercellular organic solute, while other *Thermococcus* species including *T. celer*, *T. stetteri*, and *T. zilligii* did not [31]. Furthermore, archaeal D-ProDH was previously shown to be capable of converting C4DHyp to Pyr4H2C [19]; therefore, the homologous pathway involved in the metabolism of T4LHyp by bacteria may also be operative in *T. litoralis* [7, 8]. In another hypothesis, Pyr5C was suggested to be spontaneously tautomerized to L-glutamate γ -semialdehyde via a “5-hydroxy-L-proline” intermediate (Fig. 1A). If TlProR is also able to epimerize 5-hydroxy-L-proline to the D-enantiomer due to broad substrate specificity, D-glutamate is finally produced via D-glutamate γ -semialdehyde. In bacteria, D-glutamate was reported to be produced from L-glutamate by glutamate racemase (EC 5.1.1.3), and used as a building block of cell-wall peptidoglycan [32]. Although D-glutamate has also been detected in several archaea, the homolog from archaea functions as an aspartate racemase (EC 5.1.1.13) [33]. Therefore, TlProR may be involved in an alternative pathway of D-glutamate biosynthesis. The development of the gene disruption of *T. litoralis* will be useful for understanding the physiological role(s) of the *TlProR* gene in more detail.

Supporting Information

S1 Table. Primers used in this study. ^aLower case letters indicate additional bases for introducing the digestion sites of restriction enzymes in parentheses. ^bOnly sense primers are shown. Underlining indicates mutated regions. (PDF)

Acknowledgments

We thank Dr. Takenori Satomura (University of Fukui, Japan) and Dr. Hiroshi Sekiya (Matsuyama University, Japan) for the gift of L-ProDH from *A. pernix* and D-ProDH from *P. islandicum*, and genomic DNA of *C. difficile* 630, respectively. Our thanks extend especially to Mr. Masashi Yoshida (Shinwa Chemical Industries, Kyoto, Japan) for his help in the HPLC analysis of chiral proline derivatives.

Author Contributions

Conceived and designed the experiments: SW. Performed the experiments: SW YT. Analyzed the data: SW HN. Contributed reagents/materials/analysis tools: SW YW. Wrote the paper: SW.

References

1. Wu G, Bazer FW, Burghardt RC, Johnson GA, Kim SW, Knabe DA, et al. Proline and hydroxyproline metabolism: implications for animal and human nutrition. *Amino Acids*. 2011; 40: 1053–1063. doi: [10.1007/s00726-010-0715-z](https://doi.org/10.1007/s00726-010-0715-z) PMID: [20697752](https://pubmed.ncbi.nlm.nih.gov/20697752/)
2. Bouillaut L, Self WT, Sonenshein AL. Proline-dependent regulation of *Clostridium difficile* Stickland metabolism. *J Bacteriol*. 2013; 195: 844–854. doi: [10.1128/JB.01492-12](https://doi.org/10.1128/JB.01492-12) PMID: [23222730](https://pubmed.ncbi.nlm.nih.gov/23222730/)
3. Jackson S, Calos M, Myers A, Self WT. Analysis of proline reduction in the nosocomial pathogen *Clostridium difficile*. *J Bacteriol*. 2006; 188: 8487–8495. PMID: [17041035](https://pubmed.ncbi.nlm.nih.gov/17041035/)
4. Chamond N, Grégoire C, Coatnoan N, Rougeot C, Freitas-Junior LH, da Silveira JF, et al. Biochemical characterization of proline racemases from the human protozoan parasite *Trypanosoma cruzi* and definition of putative protein signatures. *J Biol Chem*. 2003; 278: 15484–15494. PMID: [12735293](https://pubmed.ncbi.nlm.nih.gov/12735293/)
5. Reina-San-Martín B, Degraeve W, Rougeot C, Cosson A, Chamond N, Cordeiro-Da-Silva A, et al. A B-cell mitogen from a pathogenic trypanosome is a eukaryotic proline racemase. *Nat Med*. 2000; 6: 890–897. PMID: [10932226](https://pubmed.ncbi.nlm.nih.gov/10932226/)
6. Chamond N, Cosson A, Coatnoan N, Minoprio P. Proline racemases are conserved mitogens: characterization of a *Trypanosoma vivax* proline racemase. 2009; *Mol Biochem Parasitol*. 165: 170–179. doi: [10.1016/j.molbiopara.2009.02.002](https://doi.org/10.1016/j.molbiopara.2009.02.002) PMID: [19428664](https://pubmed.ncbi.nlm.nih.gov/19428664/)
7. Watanabe S, Yamada M, Ohtsu I, Makino K. α -Ketoglutaric semialdehyde dehydrogenase isozymes involved in metabolic pathways of D-glucarate, D-galactarate and hydroxy-L-proline: molecular and metabolic convergent evolution. *J Biol Chem*. 2007; 282: 6685–6695. PMID: [17202142](https://pubmed.ncbi.nlm.nih.gov/17202142/)
8. Watanabe S, Morimoto D, Fukumori F, Shinomiya H, Nishiwaki H, Kawano-Kawada M, et al. Identification and characterization of D-hydroxyproline dehydrogenase and Δ^1 -pyrroline-4-hydroxy-2-carboxylate deaminase involved in novel L-hydroxyproline metabolism of bacteria: metabolic convergent evolution. *J Biol Chem*. 2012; 287: 32674–32688. PMID: [22833679](https://pubmed.ncbi.nlm.nih.gov/22833679/)
9. Visser WF, Verhoeven-Duif NM, de Koning TJ. Identification of a human *trans*-3-hydroxy-L-proline dehydratase, the first characterized member of a novel family of proline racemase-like enzymes. *J Biol Chem*. 2012; 287: 21654–21662. doi: [10.1074/jbc.M112.363218](https://doi.org/10.1074/jbc.M112.363218) PMID: [22528483](https://pubmed.ncbi.nlm.nih.gov/22528483/)
10. Watanabe S, Tanimoto Y, Yamauchi S, Tozawa Y, Sawayama S, Watanabe Y. Identification and characterization of *trans*-3-hydroxy-L-proline dehydratase and Δ^1 -pyrroline-2-carboxylate reductase involved in *trans*-3-hydroxy-L-proline metabolism of bacteria. *FEBS Open Bio*. 2014; 4: 240–250. doi: [10.1016/j.fob.2014.02.010](https://doi.org/10.1016/j.fob.2014.02.010) PMID: [24649405](https://pubmed.ncbi.nlm.nih.gov/24649405/)
11. Watanabe S, Tozawa Y, Watanabe Y. Ornithine cyclodeaminase/ μ -crystallin homolog from hyperthermophilic archaeon *Thermococcus litoralis* functions as a novel Δ^1 -pyrroline-2-carboxylate reductase involved in putative *trans*-3-hydroxy-L-proline metabolism. *FEBS Open Bio*. 2014; 4: 617–626. doi: [10.1016/j.fob.2014.07.005](https://doi.org/10.1016/j.fob.2014.07.005) PMID: [25161870](https://pubmed.ncbi.nlm.nih.gov/25161870/)
12. Buschiazzo A, Goytia M, Schaeffer F, Degraeve W, Shepard W, Grégoire C, et al. Crystal structure, catalytic mechanism, and mitogenic properties of *Trypanosoma cruzi* proline racemase. *Proc Natl Acad Sci U S A*. 2006; 103: 1705–1710. PMID: [16446443](https://pubmed.ncbi.nlm.nih.gov/16446443/)
13. Goytia M, Chamond N, Cosson A, Coatnoan N, Hermant D, Berneman A, et al. Molecular and structural discrimination of proline racemase and hydroxyproline-2-epimerase from nosocomial and bacterial pathogens. *PLoS One*. 2007; 2: e885. PMID: [17849014](https://pubmed.ncbi.nlm.nih.gov/17849014/)
14. Finlay TH, Adams E. Kinetic and structural studies of hydroxyproline 2-epimerase. *J Biol Chem*. 1970; 245: 5248–5260. PMID: [5469165](https://pubmed.ncbi.nlm.nih.gov/5469165/)

15. Neuner A, Jannasch HW, Belkin S, Stetter KO. *Thermococcus litoralis* sp. nov.: a new species of extremely thermophilic marine archaeobacteria Arch Microbiol. 1990; 153: 205–207.
16. Sambrook J, Fritsch EF, Maniatis T. Molecular Cloning: a Laboratory Manual, 3rd ed. Cold Spring Harbor, NY: Cold Spring Harbor Laboratory; 2001.
17. Lowry OH, Rosebrough NJ, Farr AL, Randall RJ. Protein measurement with the folin phenol reagent. J Biol Chem. 1951; 193: 265–275. PMID: [14907713](#)
18. Laemmli UK. Cleavage of structural proteins during the assembly of the head of bacteriophage T4. Nature. 1970; 227: 680–685. PMID: [5432063](#)
19. Satomura T, Kawakami R, Sakuraba H, Ohshima T. Dye-linked D-proline dehydrogenase from hyperthermophilic archaeon *Pyrobaculum islandicum* is a novel FAD-dependent amino acid dehydrogenase. J Biol Chem. 2002; 277: 12861–12867. PMID: [11823469](#)
20. Sakuraba H, Satomura T, Kawakami R, Kim K, Hara Y, Yoneda K, et al. Crystal structure of novel dye-linked L-proline dehydrogenase from hyperthermophilic archaeon *Aeropyrum permix*. J Biol Chem. 2012; 287: 20070–20080. doi: [10.1074/jbc.M111.319038](#) PMID: [22511758](#)
21. Watanabe S, Hiraoka Y, Endo S, Tanimoto Y, Tozawa Y, Watanabe Y. An enzymatic method to estimate the content of L-hydroxyproline. J Biotechnol. 2015 doi: [10.1016/j.jbiotec.2015.01.026](#)
22. Penning TM, Jez JM. Enzyme redesign. Chem Rev. 2001; 101: 3027–3046. PMID: [11710061](#)
23. Kawakami R, Sakuraba H, Tsuge H, Goda S, Katunuma N, Ohshima T. A second novel dye-linked L-proline dehydrogenase complex is present in the hyperthermophilic archaeon *Pyrococcus horikoshii* OT-3. FEBS J. 2005; 272: 4044–4054. PMID: [16098188](#)
24. Kawakami R, Sakuraba H, Ohshima T. Gene and primary structures of dye-linked L-proline dehydrogenase from the hyperthermophilic archaeon *Thermococcus profundus* show the presence of a novel heterotetrameric amino acid dehydrogenase complex. Extremophiles. 2004; 8: 99–108. PMID: [15064976](#)
25. Berneman A, Alves-Ferreira M, Coatnoan N, Chamond N, Minoprio P. Medium/high throughput D-amino acid oxidase colorimetric method for determination of D-amino acids. application for amino acid racemases. J Microbial Biochem Technol. 2010; 2: 139–146.
26. Zhao S, Sakai A, Zhang X, Vetting MW, Kumar R, Hillerich B, et al. Prediction and characterization of enzymatic activities guided by sequence similarity and genome neighborhood networks. Elife. 2014; 3: e03275.
27. Madern D, Ebel C, Zaccai G. Halophilic adaptation of enzymes. Extremophiles. 2000; 4: 91–98. PMID: [10805563](#)
28. White CE, Gavina JM, Morton R, Britz-McKibbin P, Finan TM. Control of hydroxyproline catabolism in *Sinorhizobium meliloti*. Mol Microbiol. 2012; 85: 1133–1147. doi: [10.1111/j.1365-2958.2012.08164.x](#) PMID: [22804907](#)
29. Akanuma S, Nakajima Y, Yokobori S, Kimura M, Nemoto N, Mase T, et al. Experimental evidence for the thermophilicity of ancestral life. Proc Natl Acad Sci U S A. 2013; 110: 11067–11072. doi: [10.1073/pnas.1308215110](#) PMID: [23776221](#)
30. Jensen RA. Enzyme recruitment in evolution of new function. Annu Rev Microbiol. 1976; 30: 409–425. PMID: [791073](#)
31. Lamosa P, Martins LO, Da Costa MS, Santos H. Effects of temperature, salinity, and medium composition on compatible solute accumulation by *Thermococcus* spp. Appl Environ Microbiol. 1998; 64: 3591–3598. PMID: [9758772](#)
32. Fisher SL. Glutamate racemase as a target for drug discovery. Microb Biotechnol. 2008; 1: 345–360. doi: [10.1111/j.1751-7915.2008.00031.x](#) PMID: [21261855](#)
33. Long Z, Lee JA, Okamoto T, Sekine M, Nimura N, Imai K, et al. Occurrence of D-amino acids and a pyridoxal 5'-phosphate-dependent aspartate racemase in the acidothermophilic archaeon, *Thermoplasma acidophilum*. Biochem Biophys Res Commun. 2001; 281: 317–321. PMID: [11181048](#)